JOURNAL OF MATERIALS SCIENCE 22 (1987) 2192–2198

Production of ultra-fine silicon powder by the arc plasma method

K. TANAKA, K. ISHIZAKI, S. YUMOTO, T. EGASHIRA
Department of Mechanical Engineering, The Technological University of Nagaoka, Nagaoka, Niigata 940-21, Japan

M. UDA
Powder Technology Division, National Research Institute for Metals, Nakameguro, Tokyo 153, Japan

A method of producing ultra-fine silicon powder is described. The most probable particle size produced by this method was estimated to be about 30 nm by TEM observation and X-ray diffraction. The powder was produced by an arc plasma method. This method is quite feasible for bulk continuous production of ultra-fine powder. Mechanisms of the production of the powder are also discussed. The principal mechanism for this ultra-fine powder production is attributed to the increase of the partial pressure of nitrogen (or hydrogen) gas by an arc plasma.

1. Introduction

Recent technological advancement demands new materials for critical usage, such as high-temperature applications. One of the methods of obtaining new materials of better properties at high temperatures is to produce refractory materials from ultra-fine powder.

Silicon nitride and silicon carbide are excellent materials because of their strong mechanical properties at high temperatures, as well as for their strong corrosion resistance. Wide applications are expected for these substances, such as turbine blades, diesel engine parts and nuclear reactor materials. The demand for these materials is increasing day by day; for instance, the production of silicon nitride has tripled in less than three years [1]. Ultra-fine silicone powder is a good raw material for producing them. As an example, the powder is mixed with carbon powder to produce sintered silicon carbide. This process is called "Self-combustion sintering" by a group at Osaka University [2, 3].

Spherical fine silicon powder has the best sintering properties. In the present work spherical ultra-fine silicon powder of 20 to 40 nm was produced by an arc plasma method [4–8]. This method may enable the production of bulk spherical fine silicon powder on a commercial basis.

2. Experimental procedure

A home-made arc plasma furnace was used in these experiments. A schematic diagram of the equipment is shown in Fig. 1. Metallic silicon was cut into cubes of 10 mm edge length. The chemical composition (wt %) was Si 98.1, C 0.09, P 0.01, S 0.02, Fe 0.62, Al 0.92 and Ca 0.10. The specimens were placed on a water-cooled copper anode plate in an atmosphere-controlled chamber, and heated from the top surface of the cube by an arc of constant current at 60 A for two minutes. The voltage was varied between 29 and 33 V for the gas mixture of argon 35% and hydrogen 65%, and between 19 and 21 V for the rest of the gas mixtures which are described later. The arc was generated by a tungsten inert gas (TIG) welding machine. The distance between the tungsten cathode and the anode sample was maintained in the range of 3 to 4 mm.

The chamber was evacuated to about 100 Pa more than three times to purge off air by argon before each experiment. The chamber was then filled with a gas mixture of argon–hydrogen, or argon–nitrogen, to one of two different pressures. Normal experiments were conducted under slightly higher pressure than atmospheric pressure. A low pressure of 2 kPa was used to check the pressure influence of the evaporation rate of powder.

Two different kinds of argon gas were used in this work: a higher grade of 99.999% and a normal one of 99.9%. The former is named "high-purity argon". Argon without any special specification means the latter one. The volume compositions of the gases used were of nine different kinds: 100% argon; 15, 50 and 65% hydrogen mixture with argon; and 15, 25, 45, 60 and 80% nitrogen in argon. The data above 65% of hydrogen could not be obtained, because the arc could not be stabilized for higher concentration of hydrogen in the gas mixtures. A gas mixture of 45% nitrogen and 55% argon was used to check the production rate at a pressure of 2 kPa, but the arc could not stabilize and failed to produce powder.

The same gas mixture was introduced into the chamber through the shielding gas inlet of the TIG welding machine and a normal gas entrance which is located on the opposite side-wall of the powder collecting filter as seen in Fig. 1. Silicon powder was trapped by a mullite filter which had been stabilized at 1773 K for one hour.

0022–2461/87 $03.00 + .12

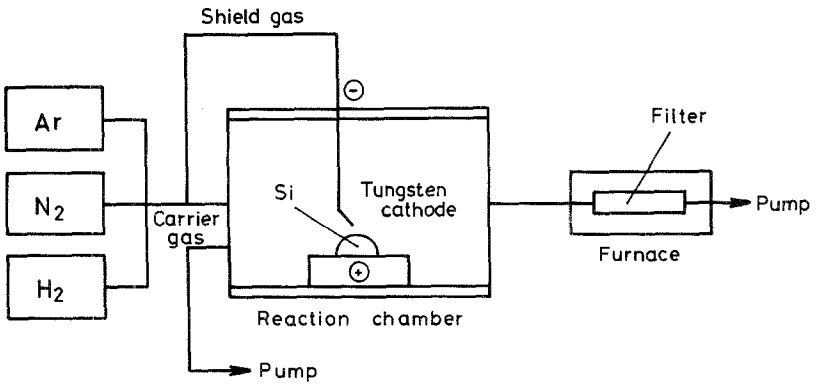

Figure 1 A metallic silicon block was placed on a water-cooled anode copper plate, and melted by a direct-current arc. The silicon powder produced was carried away by a gas mixture and collected on a mullite filter in a furnace located between the reaction chamber and a pump.

The diameters and shapes of powder particles were analysed by a TEM. A distribution of the particle size was evaluated by measuring 2000 particles. The produced powder was categorized into two groups; ultra-fine particles of 20 to 50 nm diameter, and large spattered ones of more than 10 μm diameter. These "splashed" particles were collected from the bottom of the chamber in the vicinity of the silicon metal on the anode. The production rate of ultra-fine powder was estimated from the difference of the raw material weight and the sum of the remainder and the total weight of spattered particles.

Average particle size was also estimated by X-ray diffraction. This technique is particularly applicable to metallic crystallites of sizes ranging between 3 and 50 nm. A diffraction peak is very broad and diffuse for particles smaller than 3 nm. On the other hand, the change in peak shape is insignificant for powder diameters above about 50 nm. The average particle diameter, D, is given by

$$D = \frac{K\lambda}{\beta \cos \theta} \quad (1)$$

where λ is the wavelength of the characteristic X-rays, which is in this case 0.154 18 nm for Cu$K\alpha$; θ is the Bragg angle; K is a shape factor and β is the calibrated width of the half-height of the diffraction peak. If the diffraction broadening is measured at half the maximum peak height, K takes values between 0.84 and 0.89. The latter value is for spherical particles [9]. In this work K was approximated to 0.9. The value of β is estimated using the half peak height width, b_s, of a standard silicon sample of 2.5 μm diameter, from

$$\beta^2 = b^2 - b_s^2 \quad (2)$$

where b is the width obtained from this experiment, and b_s was 2.182 radian. Typical values of b are shown in Table I.

The chemical composition of the powder was analysed by a vaporizing method, and also estimated by the measurement of X-ray diffraction intensity.

Infrared spectroscopy was used to evaluate chemical bondings of oxygen atoms. Samples were prepared from 0.5 mg ultra-fine silicon powder and 100 mg KBr powder for infrared examination. They were mechanically mixed, then pelletized under a pressure of 300 MPa.

3. Results

A typical example of the X-ray diffraction curve is shown in Fig. 2, for ultra-fine silicon powder. The produced silicon powder did not contain silicon nitride. The dissociation ratio of nitrogen gas was calculated from an equilibrium constant [10]. These results are shown in Fig. 3. Considering that nitrogen gas is 100% dissociated into the atomic form, we expected that some portion of the products may be transformed into nitride by the atomic nitrogen. Using thermodynamical data (e.g. [11]), the dissociation temperature was calculated to be about 2200 K for silicon nitride. Possibly all the silicon nitride produced may be dissociated at the high temperature outside the arc before being collected.

Fig. 4 indicates the production rates of ultra-fine powder and spattered particles against the volume fractions of gas mixtures. If the shielding gas and atmosphere contain only argon without nitrogen or hydrogen, the production of both ultra-fine powder and spattered particles is very limited.

The figure also illustrates that gas mixtures of nitrogen at 50 and 70% with argon give the maximum production rate of ultra-fine powder. The production efficiency of ultra-fine powder is about 1 mg J^{-1}, which is about three orders of magnitude better than for other methods. A system using an r.f. plasma produced about 1.8 μg J^{-1} efficiency for silicon carbide powder [12], a gas evaporation method yielded 1.7 μg J^{-1} for oxides [13], and a plasma-flame device produced iron, chromium, silicon and silicon carbide powder at rates of about 0.8, 0.6, 0.5 and 0.2 μg J^{-1}, respectively [14]. A gas mixture of hydrogen with argon allows a higher production rate of ultra-fine

TABLE I The most probable particle size, and values of b in Equation 2

Gas composition (vol %)		X-ray diffraction		Size by TEM observation (nm)
H_2	Ar	b (mrad)	Size (nm)	
65	35	4.36	38	24
25	75	3.94	44	32
60	40	3.94	44	32

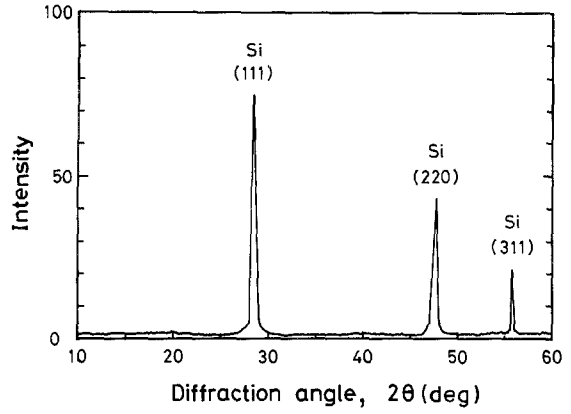

Figure 2 X-ray diffraction of the ultra-fine silicon powder produced in 60% N_2–40% Ar (99.9% purity).

particles than that of spattered particles. A possible reason of this is discussed later.

The triangle symbols in Fig. 4 indicate the evolution rates of silicon powders in 100% argon gas. The lower values of around 0.01 mg sec^{-1} correspond to argon gas at a pressure slightly higher than 0.1 MPa, and the higher values correspond to 2 kPa pressure. These generation rates of ultra-fine powder are one or two orders of magnitude lower than those obtained by using nitrogen or hydrogen mixtures. This fact shows that the arc in a nitrogen or hydrogen gas mixture is utilized not only as the heat source, but also to enhance the production mechanism of the powder. Similar kinds of gas mixture produce more or less the same amount of ultra-fine powder, as discussed elsewhere for several metals [15].

Fig. 5 represents the distribution of particle size for various gas mixtures. Three typical cases are indicated for gas mixtures of 65 vol % hydrogen and nitrogen in 35% argon, and 60% nitrogen with 40% argon. The particle size distributes sharply around 32 nm for the nitrogen and argon mixture. Slightly smaller particles – of most frequent size about 24 nm – were produced by the hydrogen and argon mixture. Typical examples of TEM observation are seen in Fig. 6.

Reasonably good agreement of particle size was also obtained by X-ray diffraction. Table I summarizes the results of the analysis. The average size by TEM observation was 6 to 14 nm smaller than that obtained by X-ray diffraction. This may be due to the

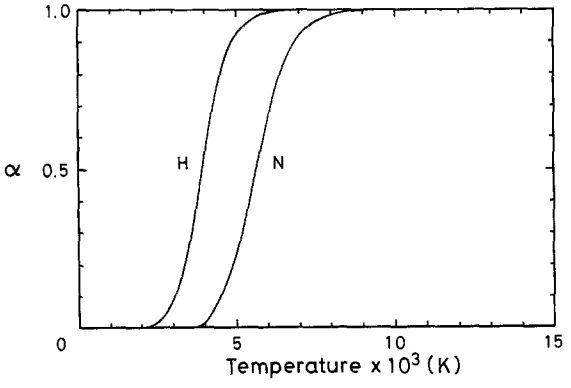

Figure 3 The dissociation ratio, α, of nitrogen and hydrogen is shown as a function of temperature. Both gases are 100% dissociated to atomic form at the arc temperature.

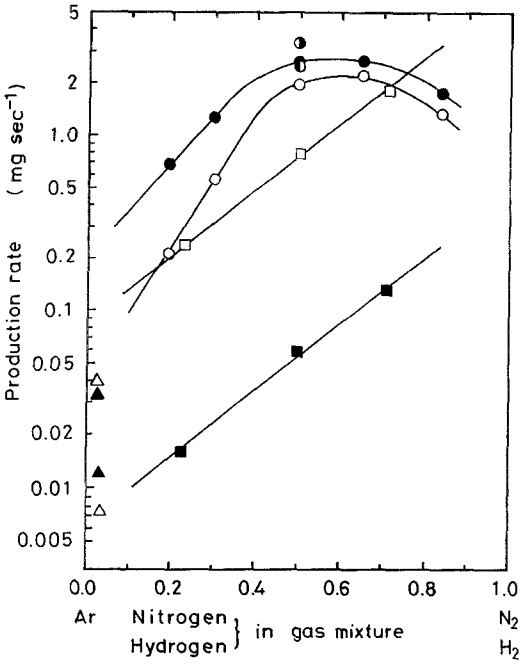

Figure 4 Production rate of powder against nitrogen or hydrogen volume percentage in argon gas for the shielding and carrier gas mixture. Open and half-open symbols indicate ultra-fine particles (≅ 20 nm); solid symbols are for spattered particles of diameter more than 10 μm. Values for 60 A arc current: (○, ●) N_2–Ar; (□, ■) H_2–Ar; (△, ▲) 100% Ar. Argon alone is not efficient to obtain ultra-fine powder. The lower production rate of about 0.01 mg sec^{-1} in 100% Ar is at a total pressure of 0.1 MPa, and the higher values are measured at 2 kPa. Gas mixtures of nitrogen at 45 to 60% result in maximum efficiency. A gas mixture of hydrogen and argon allows a higher production of ultra-fine particles than spattered particles. On increasing the arc current in N_2–Ar from 60 to (◐) 100 and (◑) 150 A the production rate of the ultra-fine powder increased proportionally.

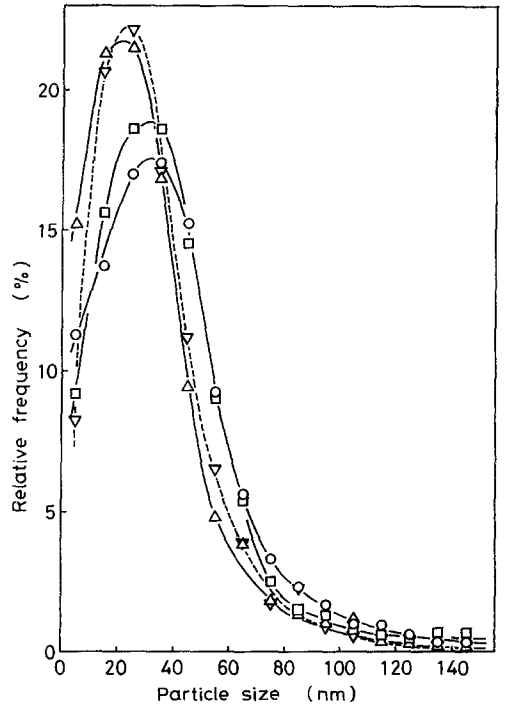

Figure 5 Distribution of particle size at 60 A arc current for 65 vol % of (△) hydrogen and (□) nitrogen in 35% argon, and (○) 60% nitrogen with 40% argon; (▽) H_2/Ar = 65/35 at 150 A current. A sharp distribution around 30 nm is obtained. This analysis was conducted for 2000 particles.

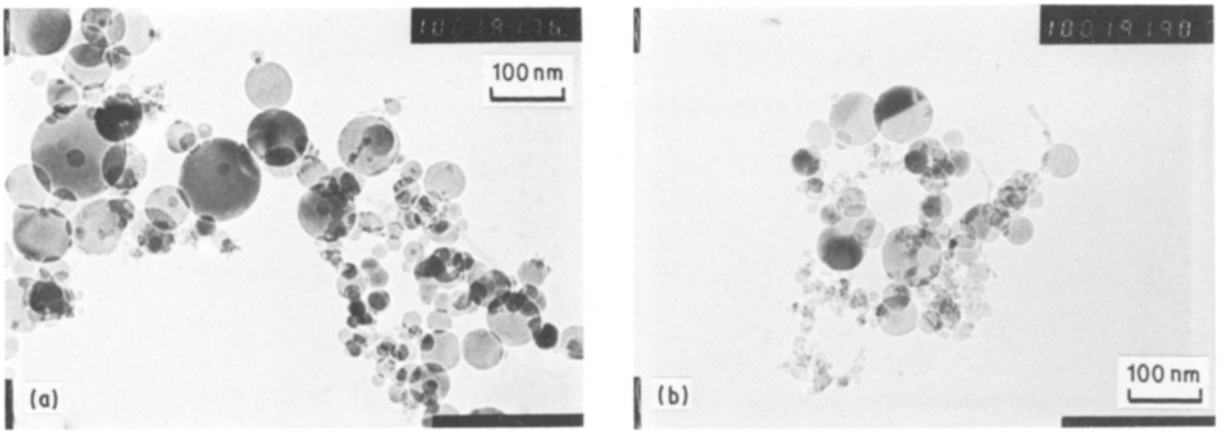

Figure 6 TEM micrograph of silicon powder produced in (a) 65% N_2–35% Ar and (b) 70% H_2–30% Ar (99.999% purity).

fact that particles were prepared for the TEM observation by mixing mechanically with alcohol. Probably smaller particles suspended more than the larger ones.

4. Discussion

Let us consider the process of the production of the powders. There are four possible mechanisms for the production which are illustrated schematically in Fig. 7.

The first process considered is normal evaporation by the heat supplied by the arc. In this mechanism, not only nitrogen gas but also pure argon gas can produce the powders. Normally the arc temperature with argon gas should rise higher than those using nitrogen or hydrogen gas. For example, Uda [5] reported 2073 K and 1873 K for the temperatures of molten iron under argon and hydrogen atmospheres, respectively. Therefore argon gas should give a better production rate than other gases, if the production mechanism of powder is assumed to be based on evaporation alone. The production rate using these bi-atomic gases such as nitrogen or hydrogen has a higher value than that using argon gas alone.

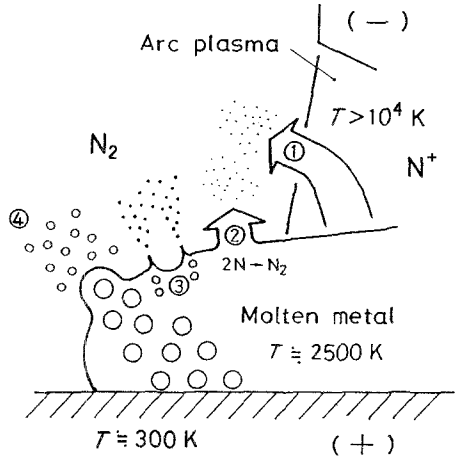

Figure 7 Schematic diagram of production mechanisms of ultra-fine silicon powder. The path 1 illustrates normal vaporization by the heat of the arc. The mechanism 2 is vaporization using the latent heat of the $2N \rightarrow N_2$ reaction. If this reaction generates bubbles a few atomic layers beneath the molten silicon surface, the bubbles splash silicon liquid in air to produce silicon particles as shown by the mechanism 3 . If the bubbles are in generated deeper locations, they splash bigger particles as indicated by the path 4 .

Therefore there must be other mechanisms than evaporation for hydrogen and nitrogen gases.

On reducing the pressure of the argon atmosphere from 0.1 MPa to 2kPa, the production rate increased from 0.008 mg sec^{-1} to 0.04 mg sec^{-1}. We may consider that the principal mechanism of powder production by argon gas alone without nitrogen or hydrogen should be that due to normal evaporation. But the contribution of this mechanism is about two orders of magnitude lower than that of other possible processes mentioned below which require a bi-atomic gas, such as nitrogen or hydrogen.

The second mechanism illustrated in the figure is also due to evaporation, but using the reaction heat of $2N \rightarrow N_2$ or $2H \rightarrow H_2$. The solubility limit of nitrogen (or hydrogen; from here on "nitrogen" represents both kinds of atom) must be extremely high, where the arc makes contact with the molten silicon. Because the molecular nitrogen is 100% dissociated in the arc, as illustrated in Fig. 3, this means that the partial pressure of nitrogen in the arc is extremely high. On the other hand, outside the arc, nitrogen atoms must recombine to form molecular nitrogen, resulting in a low nitrogen partial pressure there. This strong gradient of partial pressure induces a big difference of solubility limit in the liquid silicon between the molten metal contacts the arc and where it does not. There must be quite a strong movement of molten silicon by convection. The solute nitrogen exceeds its solubility limit when the molten metal is moved to reach the metal surface outside the arc. Hence the excess solute nitrogen atoms recombine into nitrogen molecules near the liquid surface outside the arc. This reaction emits recombination heat to enhance the silicon evaporation.

The third and fourth processes are mechanically assisted production for ultra-fine and fine powders, respectively. The aforementioned chemical reaction generates not only heat but also bubbles in the molten silicon beneath the surface. This reaction must proceed faster at a certain distance from the surface. Nearer to the liquid surface, the solute nitrogen atoms sense the lower nitrogen partial pressure. Hence the solubility limit decreases. The excess solute nitrogen atoms recombine to form molecules. But closer to the surface, the efficiency of the solute nitrogen supply is reduced, because the atoms diffuse from the molten

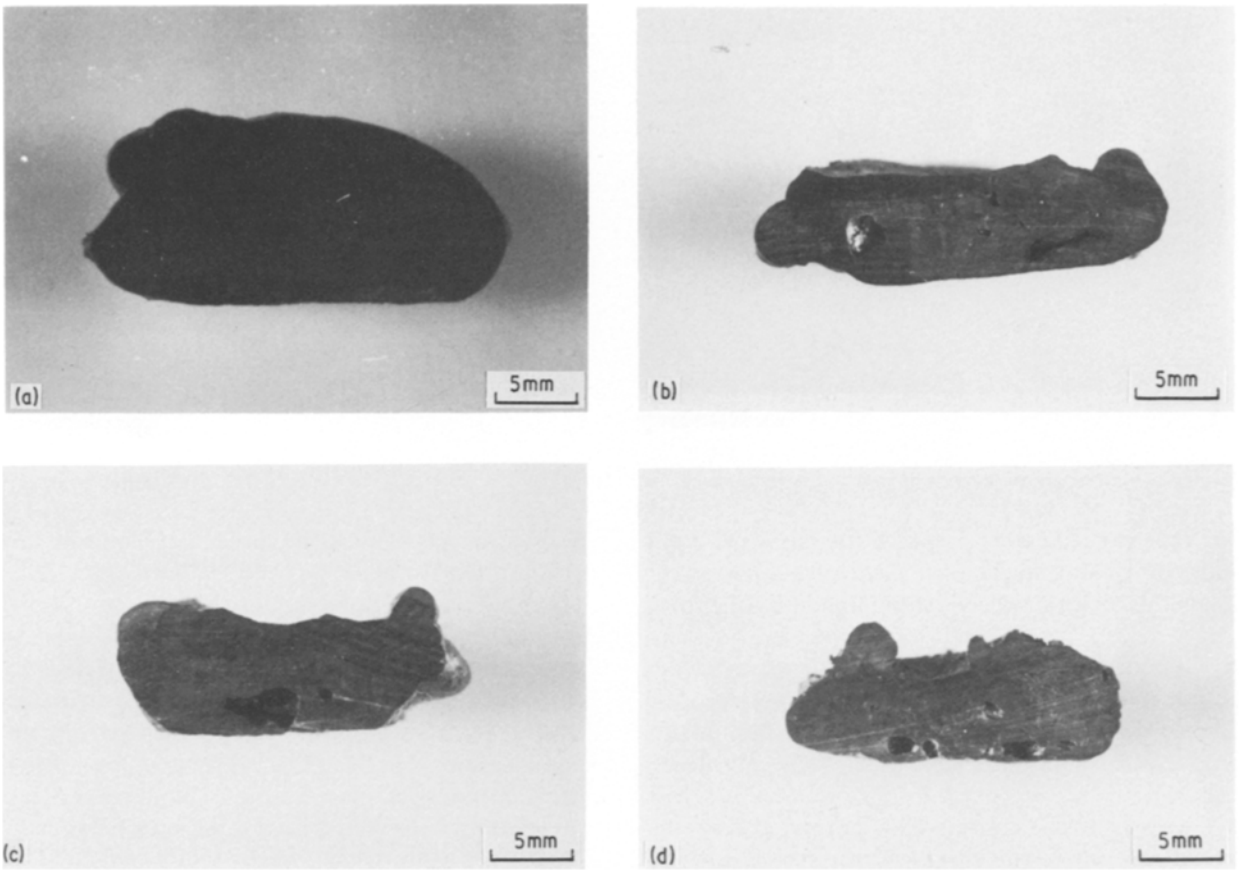

Figure 8 Section photographs of silicon samples after producing powder by arcs of (a) 100% Ar, (b) 75% Ar–25% N_2, (c) 55% Ar–45% N_2 and (d) 35% Ar–65% N_2. Big nitrogen gas bubbles of a few millimetres diameter are seen close to the water-cooled copper plate. No bubbles are observed in the sample treated by the 100% Ar arc.

surface contacting plasma to the surface outside the plasma. The authors therefore considered the optimum depth of nitrogen bubble formation. These fine bubbles splash fine molten silicon particles when they move away from the surface. This leads to the rather sharp particle size distribution. For example, if the bubbles are generated mostly at ~ 10 nm depth from the surface, they may splash liquid silicon of about 10 nm size, and these particles may grow in the gas to have a sharp distribution of 20 to 30 nm particle size, as seen in Fig. 5.

The fourth mechanism is based on the same chemical reaction as the formation of nitrogen gas. There is another reason to proceed with this recombination reaction. The molten silicon is placed on a water-cooled copper plate. The gradient of temperature from the top to the bottom of the silicon metal is huge. This slope of temperature gives a difference in the solubility limit of solute atoms. The excess solute atoms form a gas at the bottom of the liquid silicon. This kind of bubble grows to a rather bigger size, because they form at the bottom, where the temperature is low and hence the viscosity is also low, and they spatter bigger liquid silicon particles. The authors believe that this is the principal mechanism to produce splashed large particles. This is the reason why the production of spattered particles also increased by using nitrogen or hydrogen as seen in Fig. 4.

Experimental silicon metal chunks were examined after producing powder. They were cut in half by a diamond cutter, and observed as in Fig. 8. The effect of nitrogen gas is obvious. Big bubbles of a few millimetres diameter are found in those samples heated by arcs containing nitrogen in argon, and probably they contained nitrogen gas. We can see mainly those bubbles near the bottom where the samples contacted the water-cooled copper plate. This supports the aforementioned mechanism for generating spattered particles. Hydrogen atoms diffuse much faster than nitrogen. Therefore hydrogen bubbles are less effective to form bigger bubbles. Hence there are fewer spattered particles in hydrogen gas than nitrogen, as seen in Fig. 4.

The nitrogen concentration in silicon was measured after the experiments. The concentration reaches a certain value as illustrated in Fig. 9. The liquid silicon had a very high nitrogen content (2%) compared with the reported solubility limit (6×10^{-3} %) of nitrogen in molten silicon [16]. This means that silicon absorbed a higher amount of nitrogen than by Sievert's law under normal conditions of molecular nitrogen gas.

The chemical analysis of silicon powder produced by using a 70% nitrogen and 30% argon gas mixture was (wt %) N 3.98, O 12.7, Si 76.7, W 1.29, Cu 0.28, Fe 0.36, Al 2.09 and Ca 0.36. Contaminating elements such as tungsten, copper, iron, aluminium and calcium were probably from the TIG electrode. Oxygen was included as an impurity in nitrogen and argon, as well as from humidity absorbed on the surface of the furnace.

Oxygen partial pressure was measured in the chamber by a zirconia sensor which was located about 0.3 m

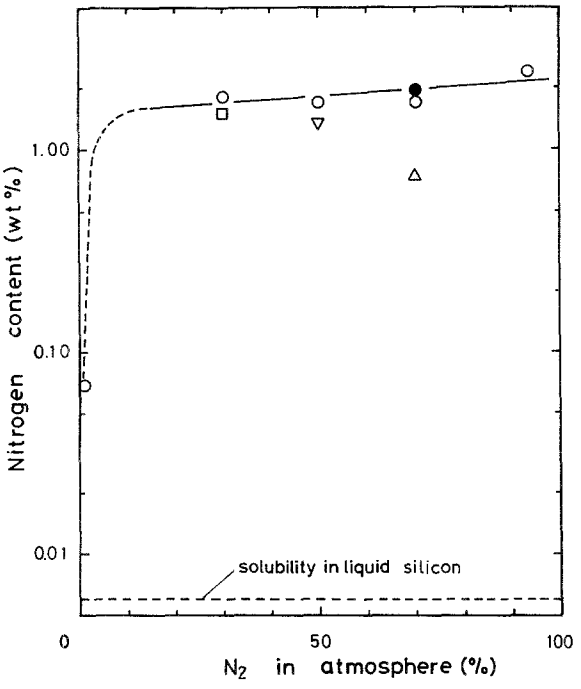

Figure 9 Nitrogen concentration (ordinate) in silicon after powder production, plotted against nitrogen concentration (abscissa) in the argon gas mixture as: (○) N_2, (□) 30% NH_3, (△) 70% N_2–5% H_2, (▽) 45% N_2–5% NH_3, (●) 70% N_2 (cooled by liquid N_2). The dotted line indicates the solubility limit at equilibrium.

away from the arc. The gas mixtures of 60% nitrogen and 40% argon contained 0.3 Pa of oxygen partial pressure at 900 K. On the other hand, the gas mixture of 70% high-purity argon and 30% hydrogen had less oxygen than the detectable limit of 1×10^{-17} Pa at 900 K. A gas mixture of 5% hydrogen showed 1×10^{-16} Pa of oxygen. Therefore the authors believe that the silicon ultra-fine powder was produced almost free of oxygen contamination.

The oxygen percentage was reduced to 6.8% from 12.7% by using a gas mixture of 70% high-purity argon (99.999%) and 30% hydrogen in the shielding gas. The surface of the resulting ultra-fine powder was oxidized during removal from the collecting chamber. The oxygen concentration of 6.8% corresponds to one or two atomic layers of coverage for the particle size of the ultra-fine powder produced, assuming that they are reasonably spherical as seen in Fig. 6.

Chemical bondings of oxygen were analysed by infrared absorption spectra as shown in Fig. 10. The ultra-fine silicon powder made in 70% nitrogen and 30% normal-grade argon shows a strong peak between 1020 and 1090 cm^{-1} which corresponds to an Si–O bond. This peak is attributed to amorphous silica, because the X-ray diffraction of the powder does not reveal the presence of silica as observed in Fig. 2. The gas mixture containing hydrogen reduces the amount of Si–O bonds, whereas the O–H bonds (around 3500 cm^{-1}) remain almost constant. The spectrum of KBr (matrix material of pellets) is also shown in the figure for comparison.

The production method described here is very easily extended and can be operated continuously to produce ultra-fine powders. The impurity control can be improved by using a better grade of gas, and by controlling the humidity absorbed on the furnace surface. This humidity can also be eliminated by continuous bulk production. For example, one of the methods of maintaining freedom from humidity is to keep the chamber wall temperature reasonably high.

5. Conclusion

The arc plasma method enables one to produce spherical silicon ultra-fine powder of about 30 nm diameter. This is the smallest silicon powder reported for possible bulk production. The optimum production rate of the gas mixture is also reported. The production efficiency was 1 mg J^{-1}, which is about three orders of magnitude higher than in other methods of producing this kind of ultra-fine powder.

Acknowledgement

The authors wish to express their gratitude to Mr Y. Nariki for his help in this work.

References

1. Dia Research Analysis Group, *Nikko Materiaru* (in Japanese) **2**(2) (1984) 95.
2. Y. MIYAMOTO, M. KOIZUMI and O. YAMADA, *J. Amer. Ceram. Soc.* **67** (1984) C224.

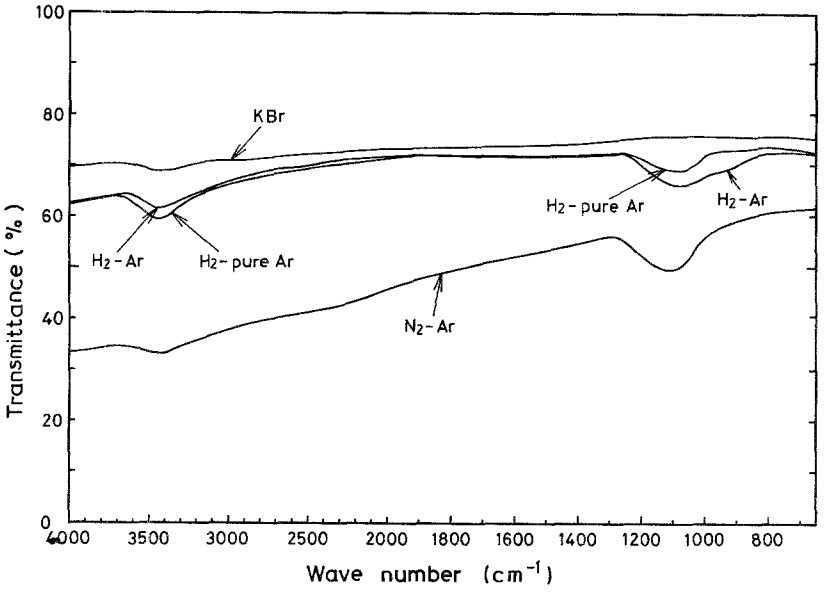

Figure 10 Infrared absorption spectra of KBr (matrix material of pellets) and ultra-fine silicon powder produced in 65% H_2–35% Ar (99.999% purity), 65% H_2–35% Ar (industrial grade), and 60% N_2–40% Ar (industrial grade). Peaks around 3500 and 1100 cm^{-1} are attributed to O–H and O–Si bonds, respectively.

3. O. YAMADA, Y. MIYAMOTO and M. KOIZUMI, *Ceram. Bull.* **64** (1985) 319.
4. M. UDA, *Trans. Natl. Res. Inst. Met.* **24** (1982) 218.
5. *Idem*, *Bull. Jpn Inst. Metals* **22** (1983) 412.
6. M. UDA and S. OHNO; "Techniques Industrieles du Japon", Bulletin de la Maison Franco-Japonaise, P.U.F. Tokyo (1984) p. 76.
7. *Idem*, *J. Chem. Soc. Jpn* **6** (1984) 862.
8. S. OHNO and M. UDA, *ibid.* **6** (1984) 924.
9. J. R. ANDERSON, "Structure of Metallic Crystals" (Academic Press, New York, 1975) p. 365.
10. Japan Chemical Society, "Kagaku Binran" (Maruzen, Tokyo, 1958) pp. 749–753.
11. L. DARKEN and R. GURRY, "Physical Chemistry of Metals" (McGraw-Hill, New York, 1953) pp. 366–370.
12. C. M. HOLLABAUGH, D. E. HULL, L. R. NEWKIRK and J. J. PETROVIK, *J. Mater. Sci.* **18** (1983) 3190.
13. M. KATO, *Jpn J. Appl. Phys.* **15** (1976) 757.
14. H. OYA, T. ICHIHASHI and N. WADA, *ibid.* **21** (1982) 554.
15. S. OHNO and M. UDA, *J. Jpn Inst. Metals* **48** (1984) 640.
16. T. NOZAKI, Y. YATSURUGI and N. AKIYAMA, IPCR Cyclotron Progress Report, Rikagaku Kenkysko (The Institute of Physical and Chemical Research), Wako, Saitama. Vol. 6 (1972) p. 106.

Received 7 August
and accepted 23 September 1986